Albedo Recovery Using a Photometric Stereo Approach

Chia-Yen Chen, Reinhard Klette *
and
Ramakrishna Kakarala †

Abstract

This paper describes a method for the estimation of surface reflectance values using a photometric stereo approach. Evaluations show that surfaces rendered with reflectance values calculated by the proposed method have more realistic appearances than those with constant albedo.

1 Introduction

A major topic in the MPEG-4 standard concerns the compression and simplification of synthetic data representations, such as surface normals, surface reflectance and texture. Although the properties can be modelled, in many situation, modelling alone is insufficient to render realistic looking objects. In many 3D visualisations, it is often necessary to render the resultant 3D model under different viewing and illumination conditions. It is imperative that the model should appear as realistic as possible. Approaches using spectral measuring devices are expensive and requires high precision manipulation. Hence it is desirable to develop alternative approaches for obtaining the surface properties to improve the appearance of rendered object.

In this work, we propose a method for the recovery of surface reflectance, i.e., the albedo values at each given surface point, using the photometric stereo method [1, 2, 6, 9].

Photometric stereo is firstly applied under the assumption of Lambertian reflectance to recover the surface normals. The calculated surface normals are used to extract the composite albedo from the input images of the object.

Experiments have shown that the surfaces rendered using calculated albedo have intensity values that are closer to that of the input images, i.e. the rendered results are more realistic than surfaces rendered using an assumed reflectance model.

*CITR, Tamaki Campus The University of Auckland, Auckland, New Zealand

†Semiconductor Products Group, Agilent Technologies, Santa Clara CA 95054 USA.

2 Model

There are three factors that influence the light reflected by a given surface; the spectral, geometric and surface factors [5]. The spectral factor describes the colours and distributions of the surface and the illuminant. The geometric factor describes the geometry of viewing and illumination directions with respect to the surface. The surface factor describes the smoothness of the surface material.

At each point $\mathbf{t}$ on a surface, there is a wavelength-dependent bidirectional reflectance distribution function (BRDF). The BRDF is defined to be the ratio of reflected radiance to the incident irradiance. At the point $\mathbf{t}$, the BRDF is a function of the incident light direction $\mathbf{s}$, the surface normal $\mathbf{n}$), the direction of view $\mathbf{v}$, and the wavelength λ:

$$\text{BRDF} = f_{\mathbf{t}}(\mathbf{s}, \mathbf{n}, \mathbf{v}, \lambda).$$

If the 3-D shape of the object is known (as measured from photometric stereo, for example), then $\mathbf{n}$ is determined for every $\mathbf{t}$. Generally, the illumination direction $\mathbf{s}$ and direction of view $\mathbf{v}$ are also known. It is only necessary to determine how $f_{\mathbf{t}}$ varies as function of λ. In what follows, we ignore the dependence on $\mathbf{t}$, $\mathbf{s}$, $\mathbf{v}$, and $\mathbf{n}$, and write simply $f(\lambda)$.

It is known from studies of human colour perception that reflectance functions may be accurately modelled (at least for purposes of our visual discrimination) by a low-order orthogonal basis expansion, i.e.,

$$f(\lambda) = \sum_{k=1}^{n} \alpha_k x_k(\lambda).$$

The basis functions $x_k(\lambda)$ have been determined [7]. Typically $n = 7$ gives an excellent fit to most surfaces, and even $n = 4$ is useful for many applications.

Suppose that the incident illumination is $E_\ell(\lambda)$. A colour camera has three types of sensors (usually red, green, and blue), with responses $r_j(\lambda)$, for $j = 1, 2, 3$. The response of the j^{th} sensor to the reflected light from illumination ℓ is

$$r_{\ell j} = \int_\lambda E_\ell(\lambda) r_j(\lambda) \sum_{k=1}^{n} \alpha_k x_k(\lambda) d\lambda.$$

1051-4651/02 $17.00 © 2002 IEEE

We can also write

$$r_{\ell j} = \sum_{k=1}^{n} \alpha_k \int_{\lambda} E_\ell(\lambda) r_j(\lambda) x_k(\lambda) d\lambda.$$

This integral involves functions which are either known, or measured independent of the object. Hence, the integral can be calculated "off-line", resulting in the expression

$$r_{\ell j} = \sum_{k=1}^{n} \alpha_k C_{\ell j k}.$$

With L light sources, a total of $3L$ responses $r_{\ell j}$ may be measured. If $3L \geq n$, then the unknown reflectance parameters α_k are determined.

In what follows, the model is discussed for $n = 1$ (scalar), and the dependence on wavelength λ is suppressed. Therefore, we write $\rho = f(\lambda)$ to denote reflectance.

3 Calculation of albedo

The Lambertian reflectance function R for a surface Z under orthographic projection can be written as

$$\begin{aligned} R(p,q) &= \eta \cos\theta_i + \sigma \\ &= E_0 \rho \cos\theta_i + \sigma \end{aligned} \quad (1)$$

where $p = \delta Z/\delta X$ and $q = \delta Z/\delta Y$ are partial derivatives of the surface Z, η is the composite albedo which combines the light source intensity E_0 and the intrinsic reflectance of surface material ρ, θ_i is the incident angle between the surface normal and light direction, and σ is the bias intensity due to background illumination, sensor calibration and quantization of irradiance values [8]. The bias intensity is assumed to be zero, such that the irradiance equation for the image intensity, E, at position (x, y) is expressed as

$$E(x,y) = E_0 \rho \cos\theta_i. \quad (2)$$

Photometric stereo is used to recover the partial surface derivatives p and q, respectively in x and y directions. Since the surface albedo values are initially unknown, an albedo independent approach, derived from Eq. 2, is employed to estimate the local surface orientations [2]. The local surface normals are calculated according to

$$\begin{aligned} \mathbf{u} = (&E_{01} E_2 |s_2| s_1 - E_{02} E_1 |s_1| s_2) \times \\ &(E_{01} E_3 |s_3| s_1 - E_{03} E_1 |s_1| s_3), \end{aligned} \quad (3)$$

where $\mathbf{u}$ is a vector collinear to the surface normal $\mathbf{n}$, E_{0i} are the light source intensities, E_i are the image irradiance values and s_i are the light source directions.

The calculated surface normals are then substituted back into the Lambertian reflectance function to find the composite albedo η using one of the three original input images. The value of η at position (x, y) is given by

$$\eta(x,y) = E_k(x,y)/\cos\theta_i \quad (4)$$

where $E_k(x, y)$ is the image intensity at position (x, y) from the k^{th} input image.

Ideally, the light source direction is constant under parallel illumination and surface points with $\theta_i > \pi/2$ will not be illuminated. However, in experimental conditions with a point light source, the scattering of illumination from the light source and the interreflections from the surface both contribute to additional illuminations. The combined effect is such that even regions with $\theta_i > \pi/2$ are illuminated, i.e. self-shadowing of the surface does not occur strictly at the $\theta_i = \pi/2$ boundary. For regions where $\cos\theta_i < 0$, i.e. the incident angle is in the range of $(-\pi, -\pi/2)$ or $(\pi/2, \pi)$, the calculated η becomes negative. However, since neither E_0 nor ρ can be negative, the equation for η can be re-written as

$$\eta(x,y) = |E(x,y)/\cos\theta_i|. \quad (5)$$

These values are taken into consideration to account for the spread of light source and the deviations in calculated surface normals. For points where the surface normals are almost perpendicular to the light source direction, values of $\cos\theta_i$ are close to 0, and the calculated η is more likely to be erroneous. Hence values from such points are eliminated by a threshold operation. The threshold can be determined independently for each situation by setting it to, say the top five percentile of all the calculated η values. Values that are larger than the threshold are discarded and remaining η values provide an estimation of the surface's reflectivity.

4 Results

Following the method mentioned, values of η are calculated for each point on the visible surface of the object.

Figure 1 shows a set of example input images for a plaster *Beethoven* head bust. For this example, the light source directions are $ls_1 = (0.27, -0.10, -1)$, $ls_2 = (0.01, 0.20, -1)$, and $ls_3 = (-0.26, -0.08, -1)$. The optical axis of the camera coincides with the z-axis of a left handed coordinate system, the horizontal and vertical axes are represented by the x and y axes respectively, and the origin of the coordinate system is defined to be in the center of the calibration sphere.

Figure 2 shows the distribution of calculated η values for the first light source. The horizontal axis represents the range of η values and the vertical axis represents the number of occurrences. The η distributions of other two light sources are similar in shape and all have peak values at around 100, with symmetric and similar spread.

The distributions of calculated η values are also consistent with in the spatial domain. For example, the face of the

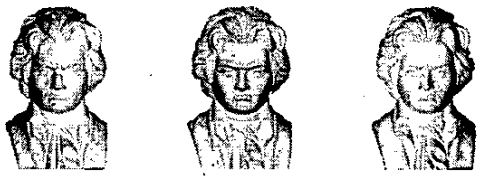

Figure 1. Examples of input images.

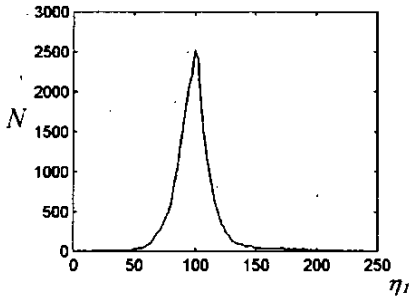

Figure 2. Distribution of calculated η values.

bust has η values of around 100 to 150, irrespective of the light source directions.

The calculated η-maps are used to render images with different light source directions. An image rendered using constant albedo is also provided. The rendered images are compared with an image taken of the original object to evaluate the effectiveness of η-maps. By visual comparison, it has been observed that the image rendered using the calculated albedo values resembles the original image of the object more than the image rendered using constant albedo values. In the given example, the surface rendered with constant albedo value appears to be more bland, with a narrower range of intensity distributions. Experiments for other light source directions yield similar results.

Table 1 compares surfaces rendered using η values calculated from three different light source directions and surface rendered using constant albedo. The errors are calculated as the sum of intensity absolute error.

From Table 1, we see that in the given example, the error between intensity values of a surface with η values obtained from ls_1 is 220384 and for ls_2 it is 174188 when the surfaces are rendered using light source direction ls_3. Both errors are much lower than when the surface is rendered using constant albedo, where the error increases by a factor of three at least.

We performed experiments with surfaces having more

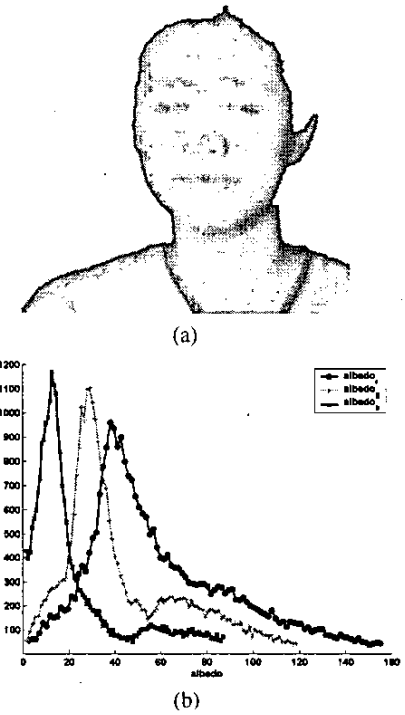

Figure 3. (a) input image for calculation of albedo, and (b) distribution of albedo values for red, green and blue channels.

complex albedo values, such as the human face. The results obtained are shown in Figs. 3 and 4. In our experiment, the rendering is performed for coloured images as well. Figure 3 shows the input image and the calculated albedo distributions for the red, green and blue colour channels.

From Fig. 4, we can see that the images rendered are consistent with the given light source direction and provide convincing visualisation for the given surface.

Errors in the rendered images shown in Fig. 4 are mainly

ls_i	η error for ls_1	η error for ls_2	η error for ls_3	constant albedo
ls_1	-	181,343	231,938	831,555
ls_2	211,847	-	219,368	781,607
ls_3	220,384	174,188	-	684,020

Table 1. Sum of absolute errors between original surface and rendered surfaces for example images.

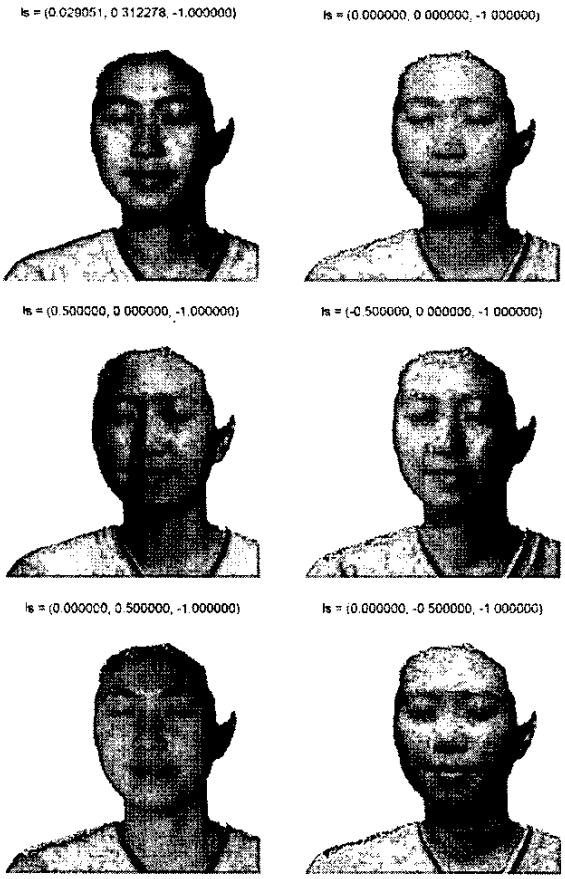

Figure 4. Images rendered using calculated albedos from different light source directions.

due to the inaccuracy in the surface values of the recovered surface and the assumption that $\sigma = 0$. Such factors cause the albedo values to be incorrectly recovered, resulting in the colour variations observed in the rendered images. In real situations, factors such as interreflection, sensor calibration and the spread of illumination will also affect the perceived surface reflectance values. In future work, we will take σ into consideration while performing albedo calculations to improve the result of calculated reflectance values.

5 Conclusions

Photometric stereo with colour imaging raises the possibility that the reflectance function itself can be estimated. Similar work has been carried out by, among others, M. D'Zmura and G. Healy at U. California (Irvine) and coworkers, and D. Greenberg at Cornell and coworkers. However, it would be of interest to build an integrated 3-D scanner which measured both shape and reflectance. We have proposed a method for albedo reconstruction using a photometric stereo approach. In our work, the composite albedo values for a given point on the surface of the object is calculated from the image irradiance and local surface orientations at that point. Experiments have been performed with surfaces with uniform albedo values, such as the plaster bust, and surfaces with complex albedo values, such as the human face. Results have shown that surfaces rendered using the calculated albedo values provide more realistic visualizations than the conventional approach.

References

[1] R. Klette, K.Schlüns: Height data from gradient fields, *Proc. of SPIE*, 2908, 1996, pp. 204-215.

[2] R. Klette, K. Schlüns and A. Koschan: *Computer Vision: Three-dimensional Data from Images*. Springer, Singapore, 1998 (German version, 1996).

[3] R. Klette, R. Kozera and K. Schlüns,: Shape from shading and photometric stereo methods, *Handbook of Computer Vision and Applications*, Vol. 2, Academic Press, San Diego, 1999, pp. 531-590.

[4] Y. Murakami, T. Obi, M. Yamaguchi, N. Ohyama and Y. Komiya: Spectral reflectance estimation from multi-band image using color chart, *Optics Communication*, vol. 188, 2001, pp. 47-54.

[5] S. Tominaga and N. Tanaka: Estimating reflection parameters from a single color image, *IEEE Computer Graphics and Applications*, vol. 20, 2000, pp. 28-66.

[6] R. J. Woodham: Photometric method for determining surface orientation from multiple images, *Optical Engineering*, vol. 19, 1980, pp. 139-144.

[7] M. J. Vrhel, R. Gershon and L. S. Iwan: Measurement and analysis of object reflectance spectra, *Color Research and Application*, vol. 19, 1994, pp. 4-9.

[8] Q. Zheng and R. Chellappa: Estimation of illuminant direction, albedo, and shape from shading, *IEEE Transaction on Pattern Analysis and Machine Intelligence*, vol. 13, 1991, pp. 680-702.

[9] R. Zhang, P. S. Tsai, J. E. Cryer and M. Shah: Shape-from-shading: a survey, *IEEE Transaction on Pattern Analysis and Machine Intelligence*, vol. 21, 1999, pp. 690-706.